

Wave Propagation Methods for Conservation Laws with Source Terms

Randall J. LeVeque and Derek S. Bale

Abstract. An inhomogeneous system of conservation laws will exhibit steady solutions when flux gradients are balanced by source terms. These steady solutions are difficult for many numerical methods (e.g., fractional step methods) to capture and maintain. Recently, a *quasi-steady wave-propagation* algorithm was developed and used to compute near-steady shallow water flow over variable topography. In this paper we extend this algorithm to near-steady flow of an ideal gas subject to a static gravitational field. The method is implemented in the software package CLAWPACK. The ability of this method to capture perturbed quasi-steady solutions is demonstrated with numerical examples.

1. Introduction

We consider the Euler equations in conservation form

$$\partial_t \mathbf{q} + \nabla \cdot \mathbf{f}(\mathbf{q}) = \psi(\mathbf{q}) \quad (1)$$

where $\mathbf{q} \in \mathbb{R}^m$ is a vector of conserved quantities, $\mathbf{f} : \mathbb{R}^m \rightarrow \mathbb{R}^m$ is the flux, and ψ is a source term due to a static gravitational field. It is well known that if \mathbf{f} is a nonlinear function of \mathbf{q} as for the Euler equations considered here, then smooth initial data may develop discontinuities in a finite time. Robust *high-resolution Godunov-type* methods have been developed that accurately capture discontinuous solutions of the one dimensional homogeneous ($\psi = 0$) version of equation (1). If $\psi \neq 0$, however, one typically uses a fractional step method in which the one dimensional analog of equation (1) is split into the artificial subproblems

$$\partial_t \mathbf{q} + \partial_x \mathbf{f}(\mathbf{q}) = 0 \quad (2)$$

$$\partial_t \mathbf{q} = \psi(\mathbf{q}), \quad (3)$$

where we have assumed quantities vary only in x . This splitting of equation (1) allows the use of high-resolution Godunov-type methods on equation (2) and powerful ODE methods on equation (3) thereby avoiding the need to incorporate the source in *Riemann problems*. These techniques work quite well for flows away from quasi-steady states.

Near steady state, however, the flux is nearly balanced by the source term so that $|\partial_t \mathbf{q}| \ll |\partial_x \mathbf{f}| \sim |\psi(\mathbf{q})|$. In order to capture this near-equilibrium flow the

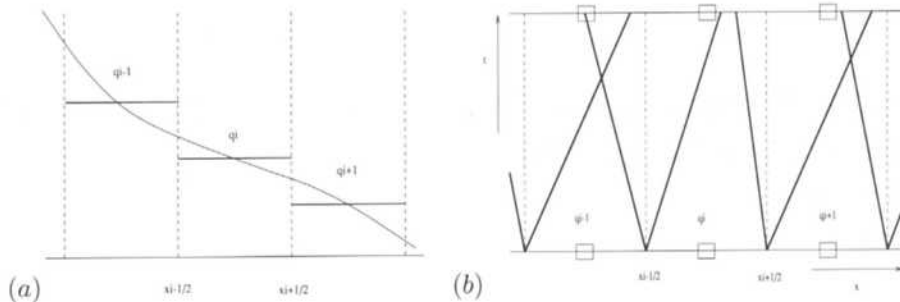


FIGURE 1. (a) standard cell averaging (b) wave propagation from cell interfaces resulting from solving the Riemann problems.

splitting method must rely on the cancellation of artificially induced dynamics. The example relevant here is a fluid in hydrostatic balance in which the flux produced by the pressure is nearly balanced by the gravitational source term. The first step of this splitting method neglects the flux term which results in a large flow due to the gravitational field. The second step neglects gravity producing a large counter flow due to the pressure forces. Small perturbations on top of this near-steady state may be lost due to the subtraction of these large and opposite flows. It is for these flows that the quasi-steady wave-propagation algorithm is used in what follows.

Recently, a *quasi-steady wave-propagation* algorithm has been developed [5] in which the source is easily incorporated into the Riemann solution used in high-resolution wave-propagation algorithms. The benefit of incorporating the source into the Riemann problems is to generate waves relevant to the quasi-steady perturbation. This algorithm was applied to shallow water flow over variable topography in [5]. A similar method has recently been proposed by Jenny and Müller [1] and discussed at this conference [2]. See [5] for references to other methods for source terms.

2. First order quasi-steady wave-propagation

Data on each time slice is represented by piecewise constant functions having the cell centered value Q_i^n at the n^{th} time level ($\Delta t \equiv k$) and in the i^{th} cell defined by $C_i \equiv [x_{i-1/2}, x_{i-1/2} + h]$ with $\Delta x \equiv h$. This representation of a function is depicted in Figure 1(a). The first order *wave-propagation* algorithm is implemented on equation (2) using a flux-difference splitting. The flux difference at the $x = x_{i-1/2}$ interface is $f(Q_i) - f(Q_{i-1})$ and is split into a right-going flux difference $\mathcal{A}^+ \Delta q_{i-1/2}$, and a left-going flux difference $\mathcal{A}^- \Delta q_{i-1/2}$. Using the notion of a

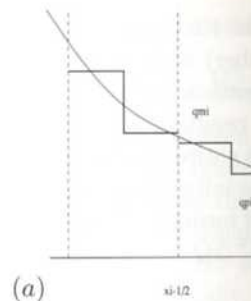


FIGURE 2. (a) centered Riemann

numerical flux function

respectively. See [4], [5] in the standard conserv

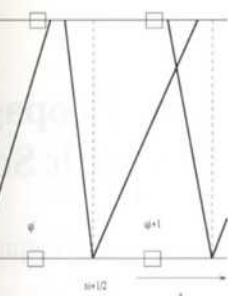
$$Q_i^{n+1}$$

It is clear that $\mathcal{A}^+ \Delta q_{i-1/2}$ problem at the left edge due to the Riemann pr being modified in this v

Now suppose that (1). The quasi-steady w a jump in the center of cell has magnitude $|Q_i^+ - Q_i^-|$ left and right half of th superscript n that deno center of the i^{th} cell is

The first criterion assu cell averages unchange the cell is updated in su Riemann problems exac

If the Courant num waves generated by th



propagation from
problems.

induced dynamics. The
which the flux produced
ce term. The first step
s in a large flow due to
ducing a large counter
op of this near-steady
d opposite flows. It is
gorithm is used in what

has been developed [5]
solution used in high-
orporating the source
ne quasi-steady pertur-
er variable topography
ny and Müller [1] and
er methods for source

t functions having the
in the i^{th} cell defined
ation of a function is
orithm is implemented
difference at the $x =$
t-going flux difference
Using the notion of a

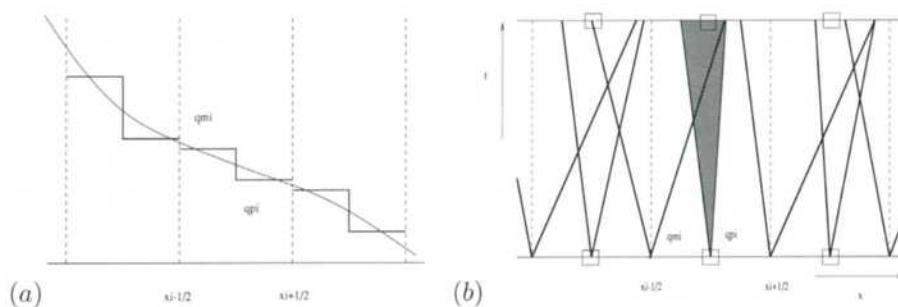


FIGURE 2. (a) modified cell values (b) wave propagation with cell centered Riemann problems included

numerical flux function we can write these left and right going flux differences as

$$\begin{aligned} \mathcal{A}^- \Delta \mathbf{q}_{i-1/2} &= \mathbf{F}_{i-1/2}^n - \mathbf{f}(\mathbf{Q}_{i-1}^n) \\ \mathcal{A}^+ \Delta \mathbf{q}_{i-1/2} &= \mathbf{f}(\mathbf{Q}_i^n) - \mathbf{F}_{i-1/2}^n, \end{aligned} \quad (4)$$

respectively. See [4], [5] for more discussion of this notation. Using these expressions in the standard conservative update gives the first order method

$$\mathbf{Q}_i^{n+1} = \mathbf{Q}_i^n - \frac{k}{h} \left(\mathcal{A}^+ \Delta \mathbf{q}_{i-1/2} + \mathcal{A}^- \Delta \mathbf{q}_{i+1/2} \right). \quad (5)$$

It is clear that $\mathcal{A}^+ \Delta \mathbf{q}_{i-1/2}$ models the flux entering the i^{th} cell due to the Riemann problem at the left edge. Similarly, $\mathcal{A}^- \Delta \mathbf{q}_{i+1/2}$ models the flux entering the cell due to the Riemann problem at the right edge. Figure 1(b) depicts the i^{th} cell being modified in this way.

Now suppose that we would like to solve the inhomogeneous conservation law (1). The quasi-steady wave-propagation algorithm is implemented by introducing a jump in the center of each cell as depicted in Figure 2(a). The jump in the i^{th} cell has magnitude $|\mathbf{Q}_i^+ - \mathbf{Q}_i^-|$ where the quantities \mathbf{Q}_i^- and \mathbf{Q}_i^+ are defined in the left and right half of that cell respectively. Here and in what follows we drop the superscript n that denotes the time level and define $\mathbf{Q}_i^{n+1} \equiv \bar{\mathbf{Q}}_i$. The jump at the center of the i^{th} cell is chosen such that the following conditions are satisfied :

$$\frac{1}{2} (\mathbf{Q}_i^- + \mathbf{Q}_i^+) = \mathbf{Q}_i \quad (6)$$

$$\mathbf{f}(\mathbf{Q}_i^+) - \mathbf{f}(\mathbf{Q}_i^-) = h\psi(\mathbf{Q}_i). \quad (7)$$

The first criterion assures that the method will remain conservative by leaving cell averages unchanged. The second, as will be demonstrated below, assures that the cell is updated in such a way that the waves emanating from the cell-centered Riemann problems exactly cancel the influence of the source.

If the Courant number is chosen to be less than 1/2 on each time slice, then waves generated by the jump located at the center of the i^{th} cell will remain

entirely within the i^{th} cell. The domain of influence for the Riemann problem at the center of the i^{th} cell (for small enough Courant number) is depicted by the shaded region of Figure 2(b). Since these cell centered Riemann problems do not influence neighboring cells, it is unnecessary to resolve the resulting flux difference $\mathbf{f}(\mathbf{Q}_i^+) - \mathbf{f}(\mathbf{Q}_i^-)$ into right and left going pieces. Rather, this entire flux difference is added into the update for $\bar{\mathbf{Q}}_i$. We must also add $k\psi(\mathbf{Q}_i)$, the influence of the source over a timestep k . If we continue to denote the influence of incoming waves at the right and left edge of the i^{th} cell by $\mathcal{A}^- \Delta Q_{i+1/2}$ and $\mathcal{A}^+ \Delta Q_{i-1/2}$ respectively, then the first order modified update becomes

$$\bar{\mathbf{Q}}_i = \mathbf{Q}_i - \frac{k}{h} (\mathcal{A}^+ \Delta Q_{i-1/2} + \mathcal{A}^- \Delta Q_{i+1/2}) + k \left[\psi(\mathbf{Q}_i) - \frac{1}{h} (\mathbf{f}(\mathbf{Q}_i^+) - \mathbf{f}(\mathbf{Q}_i^-)) \right]. \tag{8}$$

If equation (7) is satisfied then the terms in square brackets drop out and the first order update reduces to

$$\bar{\mathbf{Q}}_i = \mathbf{Q}_i - \frac{k}{h} (\mathcal{A}^+ \Delta Q_{i-1/2} + \mathcal{A}^- \Delta Q_{i+1/2}), \tag{9}$$

which is no different in form than equation (5). The piecewise constant states defining the Riemann problems, however, have changed. To see this, define $\mathbf{Q}_i^\pm = \mathbf{Q}_i \pm \delta_i$ so that criterion (6) is identically satisfied and find the solution δ_i of the algebraic system (7). Now the i^{th} Riemann problem is solved between left states $\mathbf{Q}_{i-1} + \delta_{i-1}$ and right states $\mathbf{Q}_i - \delta_i$ as depicted in Figure 2(a). These are in fact the Riemann problems arising from dynamical perturbations in the quasi-steady state. For this reason the quasi-steady wave-propagation method accurately captures quasi-steady solutions.

Although we derived this method assuming the Courant number is less than 1/2, in fact the resulting method is stable for Courant numbers up to 1 since the waves from the cell-centered Riemann problem are eliminated.

3. High resolution corrections and CLAWPACK implementation

The modified Riemann problem between states \mathbf{Q}_{i-1}^+ and \mathbf{Q}_i^- gives rise to a set of waves $\mathcal{W}_{i-1/2}^p$ (for $p = 1, 2, \dots, M_w$) with associated speeds $\lambda_{i-1/2}^p$ such that

$$\Delta \mathbf{Q}_i \equiv \mathbf{Q}_i^- - \mathbf{Q}_{i-1}^+ = \sum_{p=1}^{M_w} \mathcal{W}_i^p.$$

The first order method described above is extended to a high resolution method by adding corrections to the update (9). If we define a correction flux in terms of these waves as

$$\tilde{\mathbf{F}}_i = \frac{1}{2} \sum_{p=1}^{M_w} |\lambda_i^p| \left(1 - \frac{k}{h} |\lambda_i^p| \right) \tilde{\mathcal{W}}_i^p,$$

then the modified method

$$\mathbf{Q}_i^{n+1} = \mathbf{Q}_i^n -$$

In the above expression \mathcal{M} waves see [4], and reference

We implement the algorithm. Only the Riemann problem for components of the vector $\mathbf{Q}_i^\pm = \mathbf{Q}_i \pm \delta_i$. Finally, set left state to $\mathbf{Q}_{i-1} + \delta_{i-1}$ and applied only to the waves from the variations in the steady dynamic perturbations.

4. The Euler equations

We consider the equations for energy of an inviscid, non-heat-gravitational potential, ϕ , the

$$\partial_t (\rho \dots)$$

where $\partial_j \equiv \partial/\partial x^j$, $f^i = -\partial\phi/\partial x^i$ is the body force, ρ the mass density, \mathbf{u} the velocity, e the pressure, \tilde{u} the velocity, and e the internal energy of the fluid. For a perfect fluid $p = (\gamma - 1)\rho e$.

4.1. One Space Dimension

If the flow under consideration is such that equations (10) take the form

$$\partial_t (\rho \dots)$$

where $\tilde{\mathbf{u}} = (u, 0, 0)^T$, and $f_x = -\partial\phi/\partial x$. Note that we hesitate to write $\tilde{\mathbf{u}}$ because we allow non-uniformity in the x direction.

We would like to find δ_i such that we drop the subscript i for consistency, for example, ρ represents

the Riemann problem at number) is depicted by the Riemann problems do not the resulting flux difference is entire flux difference is the influence of the source of incoming waves at the $\mathcal{A}^+ \Delta Q_{i-1/2}$ respectively,

$$\left[-\frac{1}{h} (\mathbf{f}(\mathbf{Q}_i^+) - \mathbf{f}(\mathbf{Q}_i^-)) \right]. \quad (8)$$

ets drop out and the first

$$_{i-1/2}), \quad (9)$$

iecewise constant states To see this, define $\mathbf{Q}_i^\pm =$ find the solution δ_i of n is solved between left n Figure 2(a). These are rturbations in the quasi- gation method accurately

rant number is less than umbers up to 1 since the ated.

Implementation

\mathbf{Q}_i^- gives rise to a set of eeds $\lambda_{i-1/2}^p$ such that

high resolution method rrection flux in terms of

then the modified method takes the form

$$\mathbf{Q}_i^{n+1} = \mathbf{Q}_i^n - \frac{k}{h} (\mathcal{A}^+ \Delta \mathbf{q}_i + \mathcal{A}^- \Delta \mathbf{q}_{i+1}) - \frac{k}{h} (\tilde{\mathbf{F}}_{i+1}^n - \tilde{\mathbf{F}}_i^n).$$

In the above expression $\tilde{\mathcal{W}}^p$ is a *limited* form of \mathcal{W}^p . For details on limiting the waves see [4], and references therein.

We implement the algorithm described here in the software package CLAWPACK. Only the Riemann solvers need to be modified. First, solve equation (7) for components of the vector δ_i in each cell. Then modify the states according to $\mathbf{Q}_i^\pm = \mathbf{Q}_i \pm \delta_i$. Finally, set up data for the i^{th} Riemann problem by setting the left state to $\mathbf{Q}_{i-1} + \delta_{i-1}$ and the right state to $\mathbf{Q}_i - \delta_i$. Note that the limiters are applied only to the waves representing disturbances from the steady state, not to the variations in the steady state itself. This leads to excellent resolution of small dynamic perturbations.

4. The Euler equations

We consider the equations governing the conservation of mass, momentum, and energy of an inviscid, non-heat conducting, isotropic fluid. Coupled with a static gravitational potential, ϕ , the Euler equations take the form

$$\begin{aligned} \partial_t \rho + \partial_j (\rho u^j) &= 0 \\ \partial_t (\rho u^i) + \partial_j (\rho u^j u^i + \delta^{ij} p) &= \rho f^i \\ \partial_t e + \partial_j [(e + p) u^j] &= \rho u_j f^j, \end{aligned} \quad (10)$$

where $\partial_j \equiv \partial/\partial x^j$, $f^i = -\partial\phi/\partial x^i$, and we have made use of the Einstein summation convention in which $i, j \in \{1, 2, 3\}$. We take ρ to be the fluid density, p the pressure, \bar{u} the velocity, and e the *non-gravitational* energy made up of the kinetic and internal energy of the fluid. This system is closed with the equation of state for a perfect fluid $p = (\gamma - 1)\rho\epsilon$, where ϵ is the specific internal energy.

4.1. One Space Dimension

If the flow under consideration varies only in one direction, one can align the x -axis such that equations (10) take the one dimensional Cartesian form

$$\partial_t \rho + \partial_x (\rho u) = 0 \quad (11)$$

$$\partial_t (\rho u) + \partial_x (\rho u^2 + p) = \rho f_x \quad (12)$$

$$\partial_t e + \partial_x [(e + p) u] = \rho u f_x, \quad (13)$$

where $\bar{u} = (u, 0, 0)^T$, and $f_x = \bar{f} \cdot \bar{e}_x$ is the component of \bar{f} in the x direction. Note that we hesitate to write the standard $f_x = -g$ because we would like to emphasize that we allow non-uniform gravitational fields.

We would like to find δ_i such that equation (7) is satisfied. In what follows we drop the subscript i for conserved quantities in the i^{th} cell and it is understood that, for example, ρ represents the density in the cell under consideration. Define

$m \equiv \rho u$ and notice that the right-hand side of equation (11) is zero. Equation (7) then implies that the jump in momentum across the center of each cell must be zero. With $m^+ = m^-$, the three algebraic equations (7) reduce to a system of two algebraic equations of the form

$$\begin{aligned} \gamma \left(\frac{e^+}{\rho^+} - \frac{e^-}{\rho^-} \right) - \frac{(\gamma - 1) m^2}{2} \left[\left(\frac{1}{\rho^+} \right)^2 - \left(\frac{1}{\rho^-} \right)^2 \right] &= f_x h \\ \frac{(3 - \gamma) m^2}{2} \left(\frac{1}{\rho^+} - \frac{1}{\rho^-} \right) &= \rho f_x h, \end{aligned}$$

where we have used $p^\pm = (\gamma - 1)(e^\pm - m^2/2\rho^\pm)$ to eliminate the pressure. We now introduce the cell centered jump by defining

$$\begin{aligned} \rho^\pm &= \rho \pm \tilde{\delta}_\rho \equiv \rho (1 \pm \delta_\rho) \\ e^\pm &= e \pm \tilde{\delta}_e \equiv e (1 \pm \delta_e), \end{aligned}$$

and it is clear that for physical states we must have $\delta_\rho, \delta_e \in (-1, 1)$. In terms of δ_ρ and δ_e these equations become

$$\begin{aligned} \frac{m^2(\gamma - 3)}{\rho^2} \delta_\rho + \left[\frac{2(\gamma - 1)e}{\rho} \delta_e + f_x h \right] (1 - \delta_\rho^2) &= 0 \\ \frac{2m^2}{\rho^2} (\gamma - 1) \delta_\rho + \left[\frac{2\gamma e}{\rho} (\delta_e - \delta_\rho) + (1 - \delta_\rho^2) f_x h \right] (1 - \delta_\rho^2) &= 0. \end{aligned} \tag{14}$$

The first of equations (14) is linear in δ_e so that

$$\delta_e = \frac{m^2(3 - \gamma)}{2\rho(\gamma - 1)} \frac{\delta_\rho}{1 - \delta_\rho^2} - \frac{\rho f_x h}{2(\gamma - 1)}.$$

Using this in the second of equations (14) we get

$$m^2 \Gamma \delta_\rho + (1 - \delta_\rho^2) \left[(1 - \delta_\rho^2) f_x h - \frac{2e\delta_\rho\gamma}{\rho} - \frac{f_x h \gamma}{\gamma - 1} \right] = 0, \tag{15}$$

where $\Gamma = (\gamma^2 - \gamma + 2)/(\gamma - 1)$. Notice that this is a *fourth* order polynomial for δ_ρ that has the small parameter h in front of the δ_ρ^4 term. This singularly perturbed algebraic equation has one root that behaves as $O(1/h)$ and will be outside the interval $(-1, 1)$ for reasonable state variables. The other three roots can be sought by letting

$$\delta_\rho = \delta_\rho^0 + \delta_\rho^1 h + \delta_\rho^2 h^2 + O(h^3).$$

It turns out that two of the roots correspond to an unstable steady state and the root of interest will be

$$\delta_\rho = \frac{f_x}{(\gamma - 1)(m^2 \Gamma - 2e\gamma/\rho)} h + O(h^3). \tag{16}$$

This δ_ρ corresponds to t

$$\delta_e = -\frac{\rho f_x}{2(\gamma - 1)}$$

These solutions can be u
small perturbations, or t
equation (15). Notice tha

As an example of th
isothermal equilibrium

on the interval $0 \leq y \leq 1$
method using Strang spli
perturbing the pressure f

with $0 < \eta \ll 1$ The resu
away from this localized

In Figure 3 we have
0.25 for the Strang split
(right column) at two va
of Figure 3 and $\eta = 0.0$
figure were done on a gri
each frame represents th
a reference solution com
resolution.

In the top row of F
the truncation error of th
correct value of the pertu
maintaining the boundar
are imposing boundary c
steady method, however,
while also maintaining th
3 has an order of magniti
correct solution. However,
a better handling of interm
The fact that the quasi-ste
is another advantage.

4.2. Two Space Dimension

In the absence of a source
solves one dimensional R
quantities in a direction no

This δ_ρ corresponds to the energy shift

$$\delta_e = -\frac{\rho f_x}{2(\gamma - 1)} \left(1 - \frac{m^2(3 - \gamma)}{\rho^2(\gamma - 1)(\Gamma m^2 \rho - 2e\gamma)} \right) h + O(h^3). \quad (17)$$

These solutions can be used directly to yield a second order accurate scheme for small perturbations, or they can be used as initial guesses for a Newton solver on equation (15). Notice that an initial guess of zero momentum is unnecessary.

As an example of the method presented above, we consider a one dimensional isothermal equilibrium

$$\begin{aligned} \rho_o(y) &= p_o(y) = e^{-y} \\ u_o(y) &= 0, \end{aligned} \quad (18)$$

on the interval $0 \leq y \leq 1$. We compare the performance of a fractional step method using Strang splitting and the quasi-steady wave-propagation method by perturbing the pressure field as

$$p(t=0, y) = p_o(y) + \eta e^{-\alpha(y-y_o)^2},$$

with $0 < \eta \ll 1$. The resulting flow is essentially two acoustic pulses propagating away from this localized *small* disturbance.

In Figure 3 we have plotted the pressure perturbation $p(t, y) - p_o(y)$ at $t = 0.25$ for the Strang splitting method (left column) and the quasi-steady method (right column) at two values of η . The perturbation is $\eta = 0.001$ in the top row of Figure 3 and $\eta = 0.01$ in the bottom two frames. All computations in this figure were done on a grid of 100 cells using MC wave limiters. The dashed line in each frame represents the initial pressure perturbation. The solid line represents a reference solution computed with the quasi-steady method at a much higher resolution.

In the top row of Figure 3, the perturbation is so small that it falls below the truncation error of the splitting method, and this method fails to capture the correct value of the perturbed pressure. Notice that the split method has trouble maintaining the boundary values too. This is expected due to the fact that we are imposing boundary conditions on artificial problems (2) and (3). The quasi-steady method, however, accurately captures the dynamics of the perturbation while also maintaining the correct boundary values. The bottom row of Figure 3 has an order of magnitude larger perturbation and both methods capture the correct solution. However, the split method still has trouble at the boundary, where a better handling of intermediate boundary conditions could improve the solution. The fact that the quasi-steady method is able to handle the boundaries more easily is another advantage.

4.2. Two Space Dimensions

In the absence of a source term, the multidimensional wave-propagation algorithm solves one dimensional Riemann problems arising from the jump in conserved quantities in a direction normal to cell interfaces. A "Transverse Riemann problem"

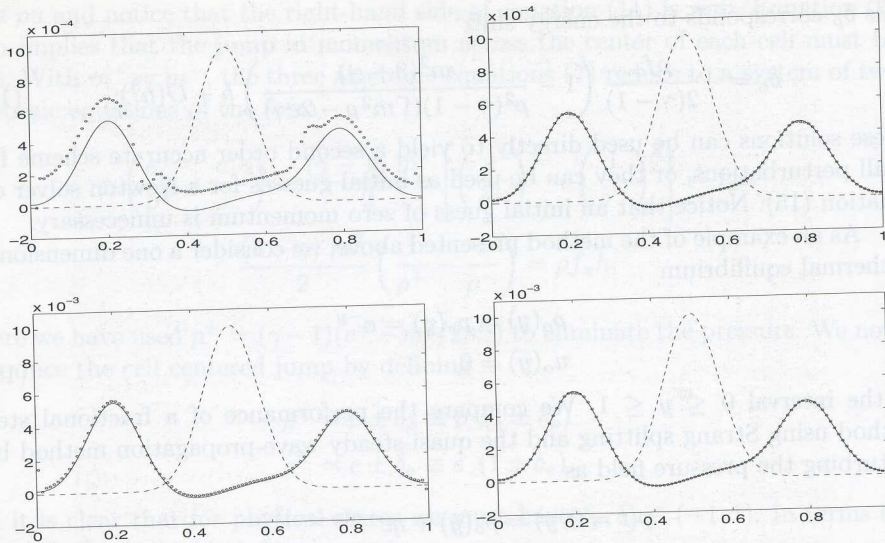


FIGURE 3. Comparison of the Strang splitting method (left column) with the quasi-steady method (right column) for two different size pressure perturbations. Top: 10^{-3} . Bottom: 10^{-2} .

is then solved to propagate these normal waves in a multidimensional manner. This gives the “corner coupling” that improves stability and accuracy (improving accuracy on smooth solutions). For details of this algorithm readers are directed to [4] and for implementation in CLAWPACK see the documentation in [3].

For the remainder of this paper we will be concerned with the two dimensional version of equations (10) so that $\vec{u} = (u^1, u^2, 0)^T$. If we consider sweeping through the grid in the x^N direction, then the equations solved to obtain the one dimensional Riemann solution are

$$\partial_t \rho + \partial_N (\rho u^N) = 0 \tag{19}$$

$$\partial_t (\rho u^N) + \partial_N (\rho (u^N)^2 + p) = \rho f^N \tag{20}$$

$$\partial_t (\rho u^T) + \partial_N (\rho u^N u^T) = 0 \tag{21}$$

$$\partial_t e + \partial_N [(e + p) u^N] = \rho u^N f^N, \tag{22}$$

where there is no sum on N or T and x^T is the transverse direction. Notice that equations (19), (20), and (22) decouple from equation (21) and yield the same one dimensional problem as dealt with in section 3. Equation (21) is an advection equation for the transverse momentum propagating at speed u^N . Here again equation (7) is solved, states are modified, and Riemann problems are solved having incorporated the source.

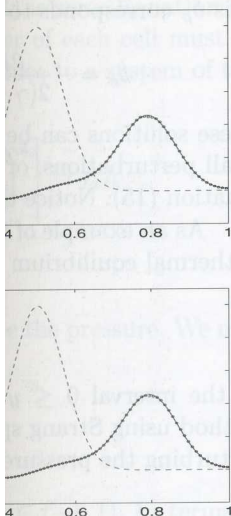
As an example of our multidimensional algorithm, consider a radially symmetric isothermal equilibrium for which the pressure is continuous across $r = r_0$,



FIGURE 4. Raydially inward. For different times a initial data in the

but the density jumps 1. This flow is in a stable e Rayleigh-Taylor instabil on the domain $[0, 1] \times [0, 1]$ computed a single quad corner is the initial den a scatter plot of the de localized ($r \approx r_0$) the m

Acknowledgement. This DMS-96226645, and DC



method (left col-
) for two differ-
n: 10^{-2} .

multidimensional manner.
and accuracy (improving
am readers are directed
mentation in [3].
ed with the two dimen-
If we consider sweeping
solved to obtain the one

- (19)
- (20)
- (21)
- (22)

verse direction. Notice
tion (21) and yield the
3. Equation (21) is an
ating at speed u^N . Here
ann problems are solved
in the absence of a sou-
consider a radially sym-
continuous across $r = r_0$,

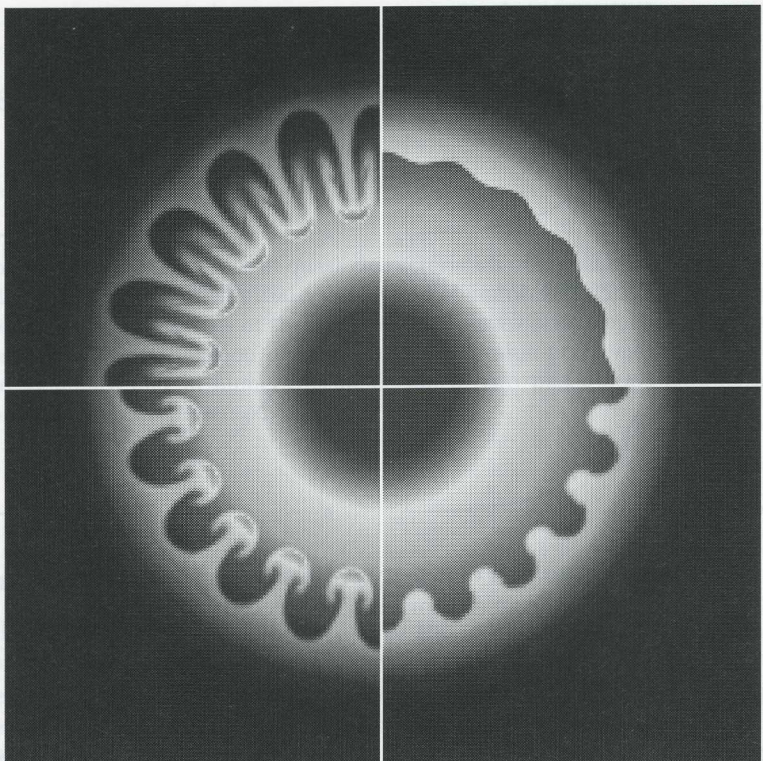


FIGURE 4. Rayleigh-Taylor instability with gravity directed radially inward. For the initial density profile see Figure 5. Four different times are shown in the four quadrants, starting with the initial data in the upper right corner and progressing clockwise.

but the density jumps by $\Delta_\rho > 0$ across $r = r_0(1 + \eta \cos(\kappa\theta))$ for $0 < \eta \ll 1$. This flow is in a stable equilibrium for all r away from r_0 , but we should expect a Rayleigh-Taylor instability at the $r = r_0$ interface. Figure 4 shows a computation on the domain $[0, 1] \times [0, 1]$ with $r_0 = 0.6$, $\Delta_\rho = 0.1$, $\kappa = 20$, and $\eta = 0.02$. We computed a single quadrant on a 120×120 grid. The image in the upper right corner is the initial density field and time progresses clockwise. Figure 5 shows a scatter plot of the density as a function of radius. Note that away from the localized ($r \approx r_0$) the method retains equilibrium and radial symmetry very well.

Acknowledgement. This work was supported in part by NSF Grants DMS-9505021, DMS-96226645, and DOE Grant DE-FG03-96ER25292.

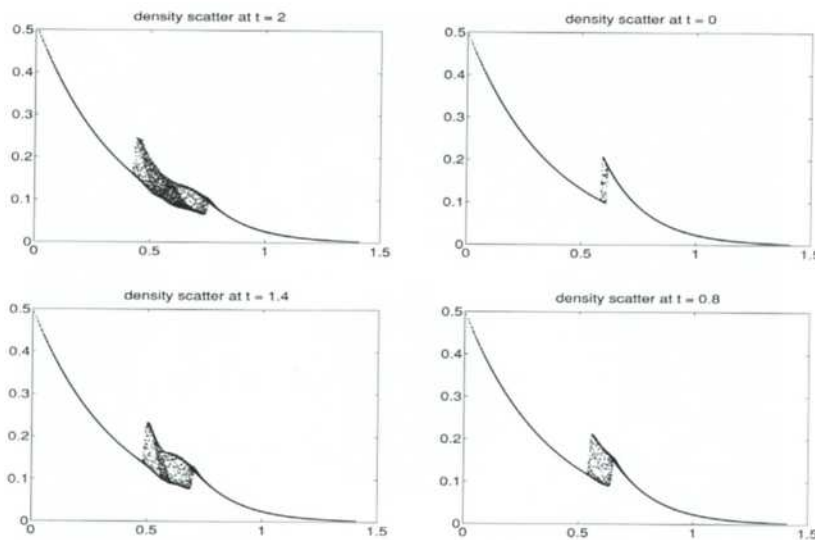


FIGURE 5. Scatter plot of density ρ_{ij} in the (i, j) cell vs. distance of the cell center from the origin. The density is shown at the same four times as in Figure 4, with the same orientation of plots.

References

- [1] P. Jenny and B. Müller, *Rankine-Hugoniot-Riemann solver considering source terms and multidimensional effects*, submitted to *J. Comput. Phys.*, (1997).
- [2] P. Jenny and B. Müller, *A new approach for a flux solver taking into account source terms, viscous and multidimensional effects*, these proceedings, (1998).
- [3] R.J. LeVeque, *CLAWPACK software*, available from netlib.bell-labs.com in netlib/pdes/claw or on the Web at the URL <http://www.amath.washington.edu/~rjl/clawpack.html>.
- [4] R.J. LeVeque, *Wave propagation algorithms for multidimensional hyperbolic systems*, *J. Comput. Phys.*, **131** (1997), 327–353.
- [5] R.J. LeVeque, *Balancing source terms and flux gradients in high-resolution Godunov methods: The quasi-steady wave-propagation algorithm*, submitted to *J. Comput. Phys.*, <ftp://amath.washington.edu/pub/rjl/papers/qsteady.ps.gz>, (1998).

Department of Applied Mathematics
 University of Washington
 Box 352420, Seattle, WA 98195-2420
 E-mail address: rjl@amath.washington.edu, dbale@amath.washington.edu

Quasi-Char

M.P. Levin

Abstract. Some
 sidered. For sol
 the hybrid mod
 posed schemes
 aerodynamics a
 porous media ar

1. Introduction

It is well-known that
 precision algorithms
 because they are ba
 However these schem
 especially in 3D cas
 schemes based on a
 in expanded charact
 an analogue of well
 interpolation proced
 marching direction a
 characteristic form a
 lines forming a region
 a short distance to ch
 in these schemes is es
 schemes and they are

2. 2D problem fo

Now we consider a pr
 example of an initial
 case

$$U_t + aU_x =$$

Here $U(t, x)$ is a sear